Role of Magnetised Crust on Torsional Shear Mode Oscillations

Debades Bandyopadhyay

Astroparticle Physics and Cosmology Division
Centre for Astroparticle Physics
Saha Institute of Nuclear Physics, Kolkata, India

Neutron rich matter and neutron stars, ECT*, Trento, 3 October, 2013

Plan of the talk

Neutron StarQuakes

- Asteroseismology is an important tool to study neutron star interior.
- Spectacular outbursts of gamma-ray flares powered by decay of the magnetic field were observed in magnetars.
- The rapidly changing field is strong enough to generate tremendous stress and breaks the crust of magnetars.
- This breaking of the crust might triggers magnetar flares and excites global seismic oscillations.
- This event is so catastrophic that it makes the whole star ringing.

Neutron stars are capable of sustaining many different types of oscillation, driven by different restoring forces:

Type	Frequency(Hz)	Sensitive to
p-mode	$\gtrsim 10^3 - 10^4$	Mean density
g-mode	$\lesssim 4 - 5$	Internal temperature
t-mode	$\gtrsim 15$	Shear strength and thickness of the crust
r-mode	~ 1	Rotation period

- Shear modes are easy to excite because the restoring force for these modes is entirely due to the relatively weak coulomb forces for the crustal ions
- These modes damp sufficiently slowly to explain durations of observed Quasiperiodic Oscillations (QPOs)
- Most importantly, the observed QPOs match expectations from models in terms of both frequency and the scaling between different harmonics.

Giant Flares

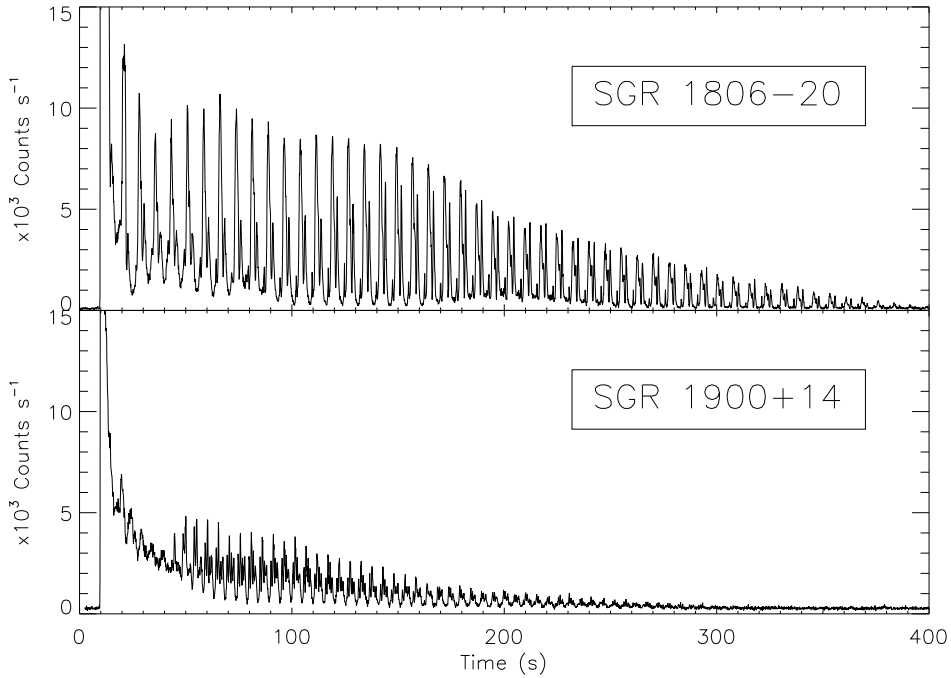

Giant flares from highly Magnetized Neutron Stars and quasiperiodic oscillations (QPOs) identified as shear modes of magnetar crusts (Strohmayer & Watts, ApJ (2005); Reddy & Watts, MNRAS (2007); Steiner & Watts, PRL (2009)). Frequencies of shear oscillations range from 18-1800 Hz.

- In the decaying tail of two such flares, SGR 1900+14 and SGR 1806-20, a number of long-lasting QPOs have been observed having frequencies 18, 26, 30, 93, 150, 625, 1838 and 28, 54, 84, 155 Hz respectively.
- Some of these frequencies are interpreted as torsional shear modes of the solid crust. Shear mode frequencies strongly depend on the shear modulus of the crust, which again is sensitive to the composition of the crust.
- Detail calculations of the composition of the crust both in strong magnetic fields have been done in some of our recent publications: J. Phys. Conf. Ser. 312 (2011) 042016 ; ApJ 736 (2011) 156; arXiv:1207.3247 as well as the work of Deibel, Steiner & Brwon arXiv:1303.3270.

So our aim is to calculate the shear mode frequencies using our magnetised crust results so that we can explain the observed QPO frequencies.

Magnetic field in NS

- Intense magnetic fields are (B$\sim 10^{12}$ G) believed to exist on the surfaces of some neutron stars. For magneters it is reported upto 10^{15}G.
- Inside the star, the magnitude of magnetic field may be even higher. The limiting interior field strength for a star is set by the virial theorem (Chandrasekhar, 1953),

$$2T + W + 3\Pi + \mathcal{M} = 0$$

$$\begin{aligned} T &= \text{total rotational kinetic energy} \\ W &= \text{gravitational potential energy} \\ \Pi &= \text{due to internal energy} \\ \mathcal{M} &= \text{magnetic energy.} \end{aligned}$$

Since T, Π small, $\mathcal{M}_{\text{max}} \sim \mathcal{W}$.

- For a star of mass M and radius R this gives

$$\frac{4\pi R^3}{3}\left(\frac{B_{\rm max}^2}{8\pi}\right) \sim \frac{GM^2}{R}$$
$$\text{or,} \quad B_{\rm max} \sim 2\times 10^8 (M/M_\odot)(R/R_\odot)^{-2}\, G$$

  For a typical neutron star of mass $M = 1.5 M\odot$ radius $R = 10$ km we have

$$B_{max} \sim 10^{18}\, G.$$

- Such high magnetic fields motivate the study of the physical properties of Neutron Star Crust in strong fields.

Outer Crust

- Outer crust begins at $\rho \sim 10^4$ g cm^{-3}
- It contains nuclei arranged in lattice (bcc) and immersed in electron gas
- In presence of magnetic fields electrons' motion perpendicular to the field gets quantized into Landau levels. It has significant effects on the composition when magnetic fields are very strong ($\gtrsim 10^{16}$) G.

Outer Crust

To find an equilibrium nucleus (A,Z), we minimize the Gibbs free energy per nucleon varying A and Z at a fixed pressure P,

$$g = \frac{E_{tot} + P}{n_b} = \frac{W_N + 4/3 W_L + Z\mu_e}{A} .$$

The total energy density is given by

$$E_{tot} = n_N(W_N + W_L) + \varepsilon_e(n_e) .$$

The energy of the nucleus (including rest mass energy of nucleons) is

$$W_N = m_n(A - Z) + m_p Z - bA ,$$

where b is the binding energy per nucleon. The lattice energy of the cell is given by

$$W_L = -\frac{9}{10}\frac{Z^2 e^2}{r_C}\left(1 - \frac{5}{9}\left(\frac{r_N}{r_C}\right)^2\right) .$$

The total pressure

$$P = P_e + \frac{1}{3} W_L n_N .$$

Baym, Pethick, Sutherland, ApJ170 (1971) 299

Effects of Strong Magnetic fields

- In presence of magnetic fields, electron motion is quantised in the plane perpendicular to the field. If field strength $B \gtrsim B_c = m_e^2/e \simeq 4.414 \times 10^{13}$G, electrons become relativistic having energy eigenvalues

$$E(\nu, p_z) = \left[p_z^2 + m_e^2(1 + 2\nu B_*)\right]^{1/2}$$

  with $\vec{B} = B\hat{z}$, $B_* = B/B_c$ and $\nu \geq 0$ is the Landau quantum number.
- The number density of electrons is (at T=0)

$$n_e = \frac{B_* m_e^2}{2\pi^2} \sum_{\nu=0}^{\nu_{max}} g_\nu p_{f_e}(\nu) \qquad g_\nu = 1 \text{ for } \nu = 0, \quad = 2 \text{ for } \nu \geq 1$$

  $p_{f_e}(\nu)$ is the maximum Z-component of momentum, ν_{max} is the maximum Landau quantum number and they are related to the electron chemical potential μ_e as

$$p_{f_e}^2(\nu) + m_e^2(1 + 2\nu B_*) = \mu_e^2, \qquad \nu_{max} = \frac{\mu_e^2 - m_e^2}{2m_e^2 B_*}$$

- Energy density and Pressure of electron gas are given as

$$\varepsilon_e = \frac{B_* m_e^2}{2\pi^2} \sum_{\nu=0}^{\nu_{max}} g_\nu \int_0^{p_{f_e}(\nu)} E(\nu, p_z) dp_z; \qquad P_e = \mu_e n_e - \varepsilon_e$$

Lai & Shapiro, ApJL 383 (1991); R. Nandi, D. Bandyopadhyay, JPCS316 (2011)

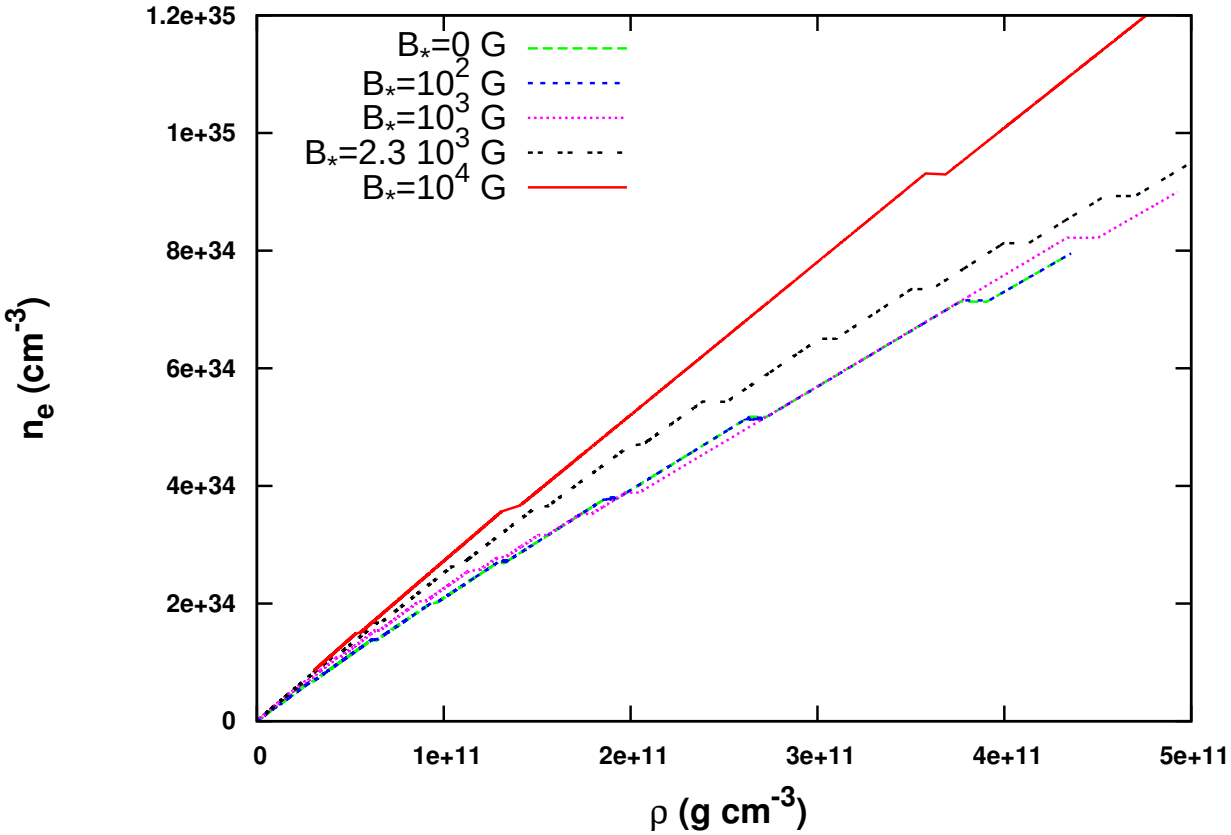

Figure: **Electron number density vs matter density at different magnetic fields,** $B_* = B/(4.414 \times 10^{13}\, G)$

Outer Crust Nuclei

Nuc	$\rho_{\max}$ (g/cm^3)						
	Z	N	$B_* = 0$	$B_* = 10^2$	$B_* = 10^3$	$B_* = 2.3\,10^3$	$B_* = 10^4$
^{56}Fe	26	30	$8.03\,10^6$	$4.68\,10^8$	$4.32\,10^9$	$9.29\,10^9$	–
^{60}Ni	28	32	–	–	–	–	$5.33\,10^{10}$
^{62}Ni	28	34	$2.72\,10^8$	$1.68\,10^9$	$1.83\,10^{10}$	$4.06\,10^{10}$	$1.31\,10^{11}$
^{64}Ni	28	36	$1.34\,10^9$	$2.78\,10^9$	$2.34\,10^{10}$	–	–
^{66}Ni	28	38	$1.50\,10^9$	–	–	–	–
^{88}Sr	38	50	–		$2.59\,10^{10}$	$6.44\,10^{10}$	$3.58\,10^{11}$
^{86}Kr	36	50	$3.10\,10^9$	$3.87\,10^9$	$4.33\,10^{10}$	$1.04\,10^{11}$	$5.37\,10^{11}$
^{84}Se	34	50	$1.06\,10^{10}$	$1.20\,10^{10}$	$6.34\,10^{10}$	$1.50\,10^{11}$	$6.61\,10^{11}$
^{82}Ge	32	50	$2.79\,10^{10}$	$2.89\,10^{10}$	$8.69\,10^{10}$	$1.99\,10^{11}$	–
^{80}Zn	30	50	$6.11\,10^{10}$	$6.18\,10^{10}$	$1.14\,10^{10}$	–	–
^{78}Ni	28	50	$9.29\,10^{10}$	$9.37\,10^{10}$	–	–	–
^{132}Sn	50	82	–	–	–	$2.39\,10^{11}$	$1.15\,10^{12}$
^{128}Pd	46	82	–	–	$1.29\,10^{11}$	$3.01\,10^{11}$	$1.42\,10^{12}$
^{126}Ru	44	82	$1.29\,10^{11}$	$1.30\,10^{11}$	$1.51\,10^{11}$	$3.50\,10^{11}$	$1.62\,10^{12}$
^{124}Mo	42	82	$1.86\,10^{11}$	$1.87\,10^{11}$	$1.73\,10^{11}$	$4.00\,10^{11}$	$1.83\,10^{12}$
^{122}Zr	40	82	$2.64\,10^{11}$	$2.63\,10^{11}$	$1.98\,10^{11}$	$4.54\,10^{11}$	$2.05\,10^{12}$
^{120}Sr	38	82	$3.77\,10^{11}$	$3.78\,10^{11}$	$4.34\,10^{11}$	$5.18\,10^{11}$	$2.32\,10^{12}$
^{118}Kr	36	82	$4.34\,10^{11}$	$4.35\,10^{11}$	$4.92\,10^{11}$	$5.53\,10^{11}$	$2.41\,10^{12}$

Inner Crust

- Inner crust of a Neutron Star begins at neutron drip point defined by $\mu_n = m_n c^2$, $\mu_n =$ neutron chemical potential.
- It contains nuclear cluster immersed in electron and neutron gas under the condition of charge neutrality ($Y_p = Y_e$) and β stability ($\mu_n = \mu_p + \mu_e$).
- The nuclear clusters are assumed to be arranged in a bcc lattice which we approximate by Wigner-Seitz cells with radius R_c.
- Electrons are extremely relativistic and can be assumed to be uniformly distributed in the cell.

BLV subtraction procedure

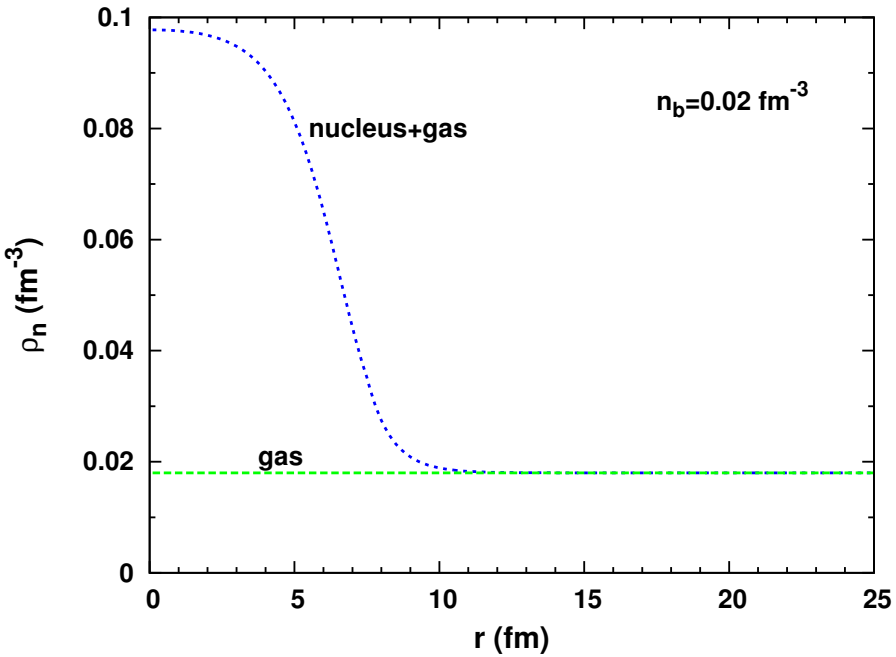

Bonche, Levit and Vauthetin
NPA 427(1984) 278

The nuclear+gas(NG) solution and the gas(G) solution coincides at large distance. This allows to define the grand potential of the nucleus as:

$$\Omega_N = \Omega_{NG} - \Omega_G$$

Grand potential is defined as

$$\Omega = \mathcal{F} - \sum_q \mu_q A_q$$

where $q = (n, p)$ and $\mathcal{F}$ is the free energy given by

$$\mathcal{F}(\langle\rho\rangle, Y_p, T) = \int [\mathcal{H}(r) - Ts(r) + \mathcal{E}_c(r) + f_e(\rho_e)]\, d\mathbf{r}.$$

$$\begin{aligned} \mathcal{H} &= \text{baryonic energy density} \\ s &= \text{entropy density of baryons} \\ \mathcal{E}_c &= \text{Coulomb energy density} \\ f_e &= \text{free energy density of electrons} = \mathcal{E}_e - Ts_e \end{aligned}$$

The energy density functional for Skyrme interaction is

$$\begin{aligned}\mathcal{H}(r) &= \frac{\hbar^2}{2m_n^*}\tau_n + \frac{\hbar^2}{2m_p^*}\tau_p + \frac{1}{2}t_0\left[\left(1+\frac{x_0}{2}\right)\rho^2 - \left(x_0+\frac{1}{2}\right)\left(\rho_n^2+\rho_p^2\right)\right] \\ &\quad -\frac{1}{16}\left[t_2\left(1+\frac{x_2}{2}\right) - 3t_1\left(1+\frac{x_1}{2}\right)\right](\nabla\rho)^2 \\ &\quad -\frac{1}{16}\left[3t_1\left(x_1+\frac{1}{2}\right) + t_2\left(x_2+\frac{1}{2}\right)\right]\left[(\nabla\rho_n)^2+(\nabla\rho_p)^2\right] \\ &\quad +\frac{1}{12}t_3\rho^\alpha\left[\left(1+\frac{x_3}{2}\right)\rho^2 - \left(x_3+\frac{1}{2}\right)\left(\rho_n^2+\rho_p^2\right)\right]\end{aligned}$$

where $\rho = \rho_n + \rho_p$ and m_q^* are the effective mass of nucleons given as

$$\begin{aligned}\frac{m}{m_q^*(r)} &= 1 + \frac{m}{2\hbar^2}\left\{\left[t_1\left(1+\frac{x_1}{2}\right) + t_2\left(1+\frac{x_2}{2}\right)\right]\rho\right. \\ &\quad \left. + \left[t_2\left(x_2+\frac{1}{2}\right) - t_1\left(x_1+\frac{1}{2}\right)\right]\rho_q\right\}.\end{aligned}$$

In the Thomas-Fermi approximation the kinetic energy density τ_q is given by

$$\tau_q(r) = \frac{3}{5}(3\pi^2)^{2/3}\rho_q^{5/3} \qquad \text{at } T = 0,$$

$$\tau_q(r) = \frac{1}{2\pi^2}\left(\frac{2m_q^* T}{\hbar^2}\right)^{5/2} J_{3/2}(\eta_q) \qquad \text{at } T \neq 0.$$

The fugacity η_q is obtained as

$$\eta_q(r) = (\mu_q - V_q(r))/T,$$

where V_q is the single-particle potential experienced by nucleons. η_q is related to nucleonic density as

$$\rho_q(r) = \frac{1}{2\pi^2}\left(\frac{2m_q^* T}{\hbar^2}\right)^{3/2} J_{1/2}(\eta_q).$$

Entropy density of the nucleons is given by

$$\begin{aligned} s(r) &= \sum_q [(5/3)J_{3/2}(\eta_q)/J_{1/2}(\eta_q) - \eta_q]\,\rho_q. \\ &= \sum_q \left[\frac{5}{3}\frac{\hbar^2}{2m_q^*}\frac{\tau_q}{T} - \eta_q \rho_q\right] \end{aligned}$$

The Coulomb energies for the NG and G phases are:

$$\begin{aligned} E_{NG}^c &= \frac{1}{2}\int (\rho_{NG}^p(r') - \rho_e)\frac{e^2}{\mid \mathbf{r} - \mathbf{r}' \mid}(\rho_{NG}^p(r) - \rho_e) d\mathbf{r} d\mathbf{r}' \\ E_G^c &= \frac{1}{2}\int (\rho_G^p(r') - \rho_e)\frac{e^2}{\mid \mathbf{r} - \mathbf{r}' \mid}(\rho_G^p(r) - \rho_e) d\mathbf{r} d\mathbf{r}' \\ &\quad + \int \rho_N^p(r')\frac{e^2}{\mid \mathbf{r} - \mathbf{r}' \mid}(\rho_G^p(r) - \rho_e) d\mathbf{r} d\mathbf{r}' \end{aligned}$$

The solutions to the density profiles can be obtained from the variational equations

$$\frac{\delta\Omega_{NG}}{\delta\rho^q_{NG}} = 0 \ \textit{and} \ \ \frac{\delta\Omega_G}{\delta\rho^q_G} = 0$$

The resulting coupled equations are

$$\begin{aligned} T\,\eta^q_{NG}(r) + V^q_{NG} + V^c_{NG}(\rho^p_{NG}, \rho_e) &= \mu_q, \\ T\,\eta^q_G(r) + V^q_G + V^c_G(\rho^p_{NG}, \rho^p_G, \rho_e) &= \mu_q. \end{aligned}$$

$V^q_{NG,G}$ are the nuclear part of the single-particle potentials and $V^c_{NG,G}$ are the corresponding Coulomb part.

Average nucleonic chemical potentials are determined as

$$\mu_q = \frac{1}{A_q}\int [T\,\eta^q_{NG}(r) + V^q_{NG}(r) + V^c_{NG}(r)]\rho^q_{NG}(r)d\mathbf{r}$$

where A_q refers to N or Z of the cell.
Now the nucleus (A_N, Z_N) is obtained as

$$\begin{aligned} Z_N &= \int \left[\rho_p^{NG}(r) - \rho_p^{G}(r)\right] d\mathbf{r} \\ N_N &= \int \left[\rho_n^{NG}(r) - \rho_n^{G}(r)\right] d\mathbf{r} \text{ and } A_N = Z_N + N_N \end{aligned}$$

Inner Crust

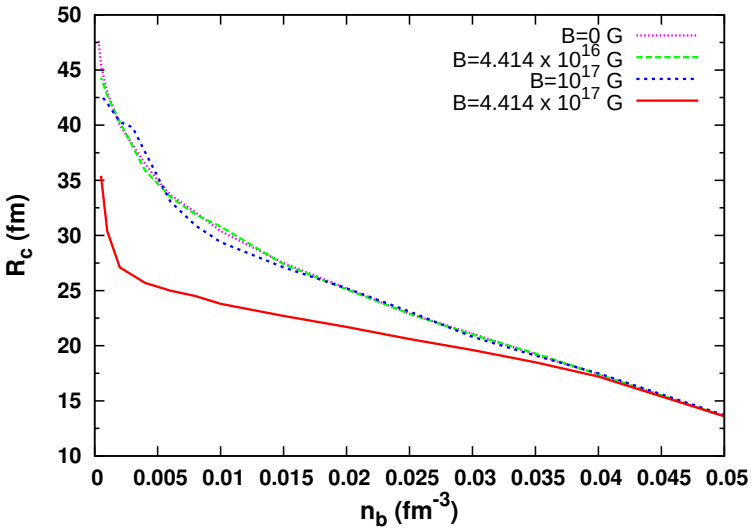

Figure: Cell radius versus baryon density

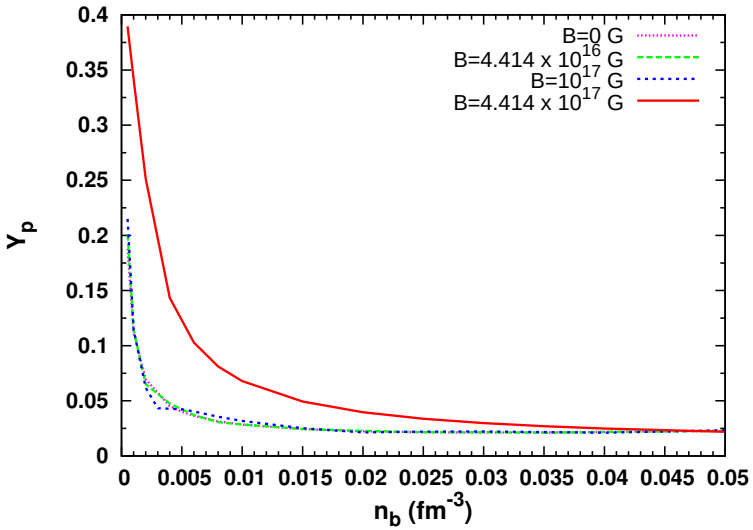

Figure: Proton fraction as a function of baryon density

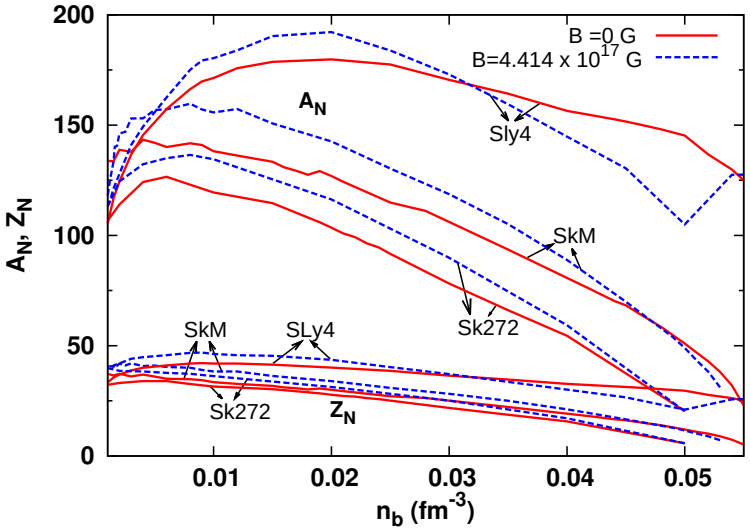

Figure: Equilibrium nuclei vs baryon density

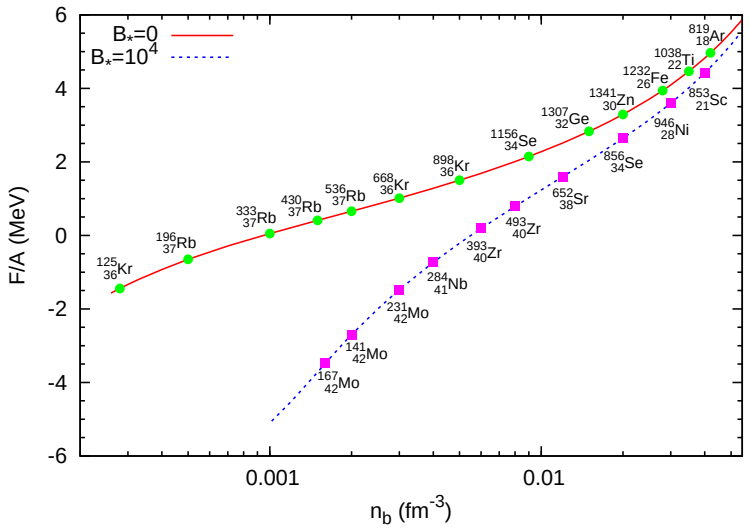

Figure: Free energy vs baryon density for SkM interaction

R. Nandi, D. Bandyopadhyay, I.N. Mishustin and W. Greiner, ApJ 736 (2011) 156

Shear Modulus

- The shear modulus of the crust is derived using a Monte Carlo simulation of the Coulomb interactions in the crust and is given by (Strohmayer et al. 1991):

$$\mu = 0.1194 \times \frac{n_i (Ze)^2}{a}$$

  Here Z is the atomic number of the ions, $n_i = n_e/Z$ is the ion density, and $a = (3/4\pi n_i)^{1/3}$ is the average inter-ion spacing.
- Z and n_e are obtained from the composition of the crust

Shear Modulus

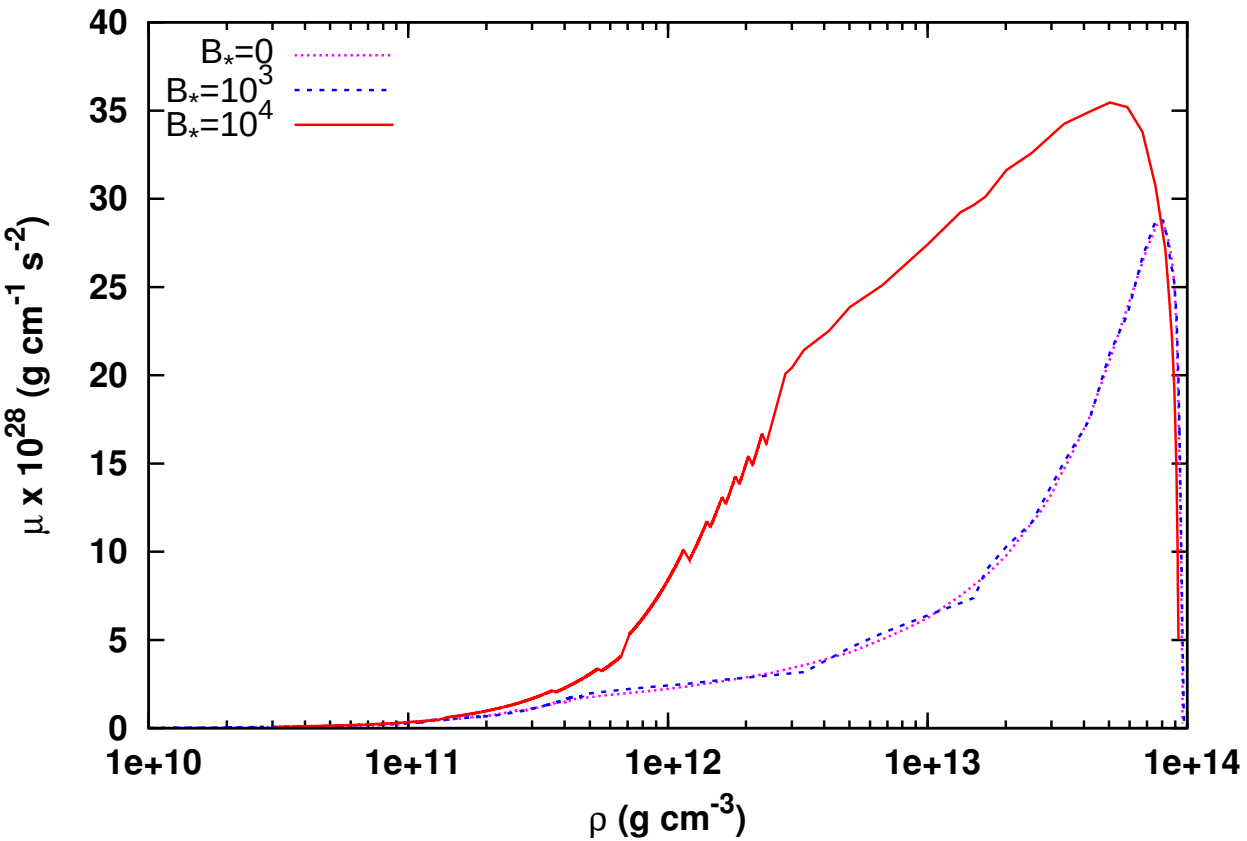

Figure: **Shear modulus vs matter density at different magnetic fields,** $B_* = B/(4.414 \times 10^{13}\, G)$

Formalism

- Shear modes are incompressible and do not result in density perturbation in the unperturbed star
- A strong dipole magnetic field is assumed to be associated with the equilibrium star
- We neglect any deformation in the star due to the magnetic field
- Equilibrium model of magnetars can be described by a spherically symmetric solutions of the TOV equations. The line element is then (Sotani et al, MNRAS 375 (2007) 261)

$$ds^2 = -e^{2\Phi}dt^2 + e^{2\Lambda}dr^2 + r^2(d\theta^2 + \sin^2\theta d\phi^2),$$

- In spherical polar coordinates, 4-potential is given by

$$A_\mu = (0, 0, 0, A_\phi).$$

with

$$A_\phi = a_{\ell_M}(r)\sin\theta\partial_\theta P_{\ell_M}(\cos\theta), \quad \ell_M = 1$$

- For the metric chosen here, Maxwell's equations $F^{\mu\nu}_{\ ;\nu} = 4\pi J^\mu$ lead to the following elliptic equation for a_1

$$e^{-2\Lambda}\frac{d^2a_1}{dr^2} + (\Phi' - \Lambda')e^{-2\Lambda}\frac{da_1}{dr} - \frac{2}{r^2}a_1 = -4\pi j_1,$$

with a form for current distribution $j_1 = f_0 r^2(\epsilon + p)$.

- In the exterior of the star

$$a_1^{(\mathrm{ex})} = -\frac{3\mu_b r^2}{8M^3}\left[\ln\left(1 - \frac{2M}{r}\right) + \frac{2M}{r} + \frac{2M^2}{r^2}\right],$$

  μ_b is the magnetic dipole moment for an observer at infinity.
- The interior solution for 'a_1' is obtained by solving the equation numerically
- Finally, the magnetic field distribution is given by

$$\begin{aligned} B_r &= \frac{2e^{\Lambda}\cos\theta}{r^2}a_1, \\ B_\theta &= -e^{-\Lambda}\sin\theta a_1'(r) \end{aligned}$$

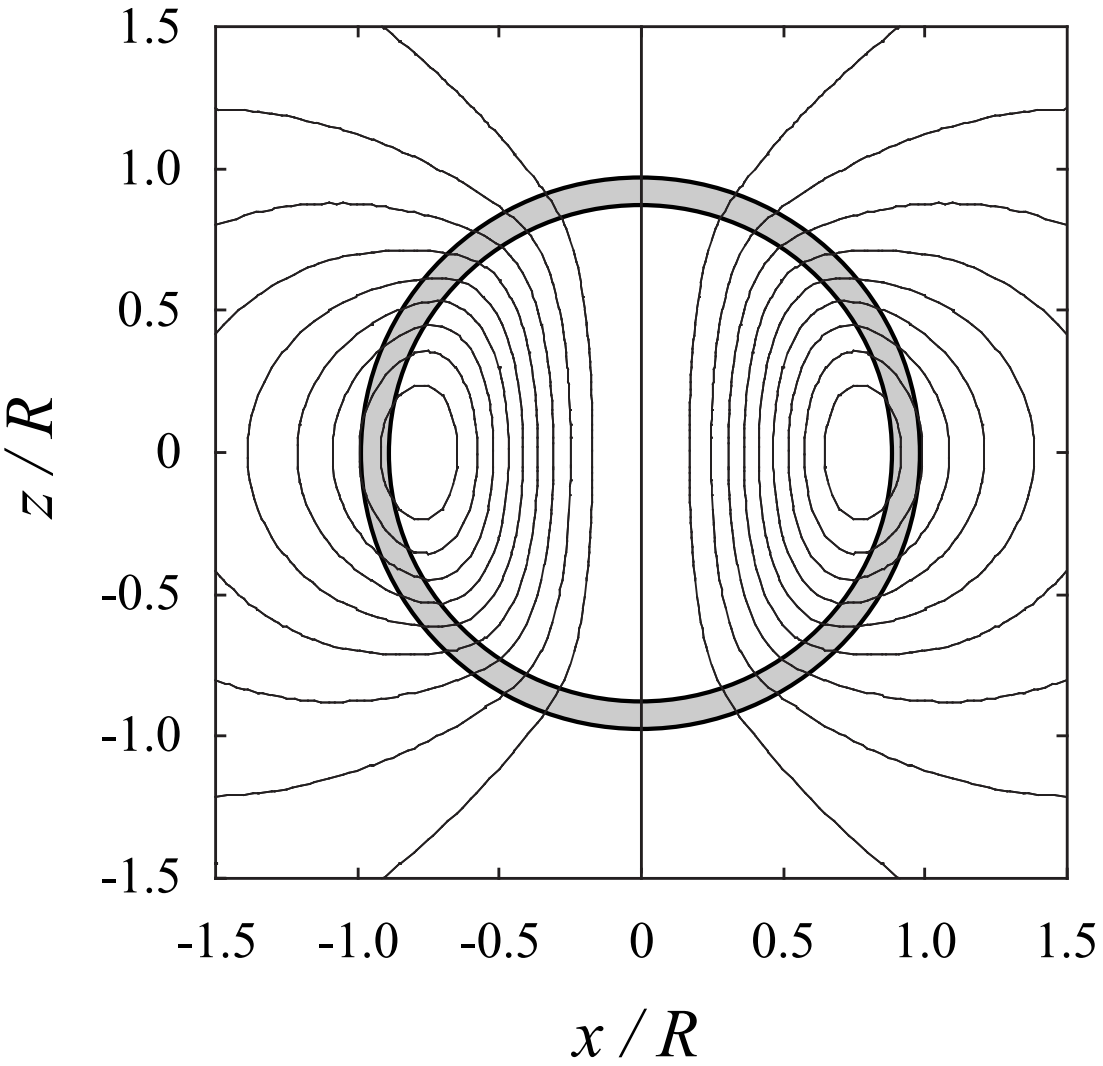

Figure: Magnetic field lines of a typical equilibrium model

Perturbed Star

- The perturbation equation describing shear mode oscillations is derived from linearized equations of motion.
- Equations of motion are obtained from the perturbed Einstein Field Equations

$$\delta(G^{\mu\nu} - 8\pi T^{\mu\nu}) = 0 \ .$$

- The stress-energy tensor of a magnetised relativistic star is

$$T^{\mu\nu} = T^{\mu\nu}_{M} + T^{\mu\nu}_{EM} \ .$$

- In the perturbed star, the coordinate location of a particle of stellar matter oscillates
- The radial and angular variation of the angular displacement of the stellar matter produce shears of the star's crystal lattice.
- One needs to provide the linearised shear stress tensor $\delta T^{\mu\nu}_{s}$

- To study oscillation modes, the linearized dynamical equations governing the magnetized fluid and crust are specialized to the case of axial perturbations.
- In general, toroidal modes are pure shear deformations, divergence-free , with no radial component.
- So, here the only non vanishing perturbed fluid variable is

$$\delta u^{\phi} = e^{-\Phi}\mathcal{Y}(r,t)\frac{1}{\sin\theta}\partial_{\theta}P_{\ell}(\cos\theta)$$

- Assuming $\mathcal{Y}(r,t) = \mathcal{Y}(r)e^{i\omega t}$, the perturbation equation becomes

$$\begin{aligned}
\left[\mu + (1+2\lambda_1)\frac{{a_1}^2}{\pi r^4}\right]\mathcal{Y}'' \quad &+ \quad \left\{\left(\frac{4}{r} + \Phi' - \Lambda'\right)\mu + \mu' + (1+2\lambda_1)\frac{a_1}{\pi r^4}\left[\left(\Phi' - \Lambda'\right)a_1 + 2{a_1}'\right]\right\}\mathcal{Y}' \\
&+ \quad \left\{\left[\left(\epsilon + p + (1+2\lambda_1)\frac{{a_1}^2}{\pi r^4}\right)e^{2\Lambda} - \frac{\lambda_1 {a_1}'^2}{2\pi r^2}\right]\omega^2 e^{-2\Phi}\right. \\
&- \quad \left.(\lambda - 2)\left(\frac{\mu e^{2\Lambda}}{r^2} - \frac{\lambda_1 {a_1}'^2}{2\pi r^4}\right) + \frac{(2+5\lambda_1)a_1}{2\pi r^4}\left\{\left(\Phi' - \Lambda'\right){a_1}' + {a_1}''\right\}\right\}\mathcal{Y} \\
&= \quad 0
\end{aligned}$$

where μ is the shear modulus in the crust and

$$\begin{aligned} \lambda &= \ell(\ell+1), \\ \lambda_1 &= -\frac{\ell(\ell+1)}{(2\ell-1)(2\ell+3)}. \end{aligned}$$

- In order to solve a system of first-order ODEs, we define new variables $\mathcal{Y}_1$ and $\mathcal{Y}_2$, through

$$\begin{aligned} \mathcal{Y}_1 &\equiv \mathcal{Y} r^{1-\ell}, \\ \mathcal{Y}_2 &\equiv \left[\mu + (1+2\lambda_1)\frac{{a_1}^2}{\pi r^4}\right] e^{\Phi-\Lambda}\mathcal{Y}' r^{2-\ell}. \end{aligned}$$

- The final first-order system of equations to be solved numerically for the eigenvalues ω is then

$$\begin{aligned} {\mathcal{Y}_1}' &= -\frac{\ell-1}{r}\mathcal{Y}_1 + \frac{\pi r^3}{\pi r^4 \mu + (1+2\lambda_1){a_1}^2} e^{-\Phi+\Lambda}\mathcal{Y}_2, \\ {\mathcal{Y}_2}' &= -\Bigg[\left(\epsilon + p + (1+2\lambda_1)\frac{{a_1}^2}{\pi r^4} - \lambda_1 e^{-2\Lambda}\frac{{a_1}'^2}{2\pi r^2}\right)\omega^2 r e^{2(\Lambda-\Phi)} \\ &\quad - (\lambda-2)\left(\frac{\mu e^{2\Lambda}}{r} - \frac{\lambda_1 {a_1}'^2}{2\pi r^3}\right) + (2+5\lambda_1)\frac{a_1 e^{2\Lambda}}{\pi r^3}\left(\frac{a_1}{r^2} - 2\pi j_1\right)\Bigg] e^{\Phi-\Lambda}\mathcal{Y}_1 - \frac{\ell+2}{r}\mathcal{Y}_2, \end{aligned}$$

Boundary Conditions

- The horizontal traction ($t_i = n_j \sigma_{ji}$) must be zero at the top and bottom of the crust. These leads to the condition

$$\mathcal{Y}_2(r_i) = 0, \qquad r_i = R_c, R$$

- We also use the normalization condition

$$\mathcal{Y}_1(R) = 1$$

Fundamental Shear Modes

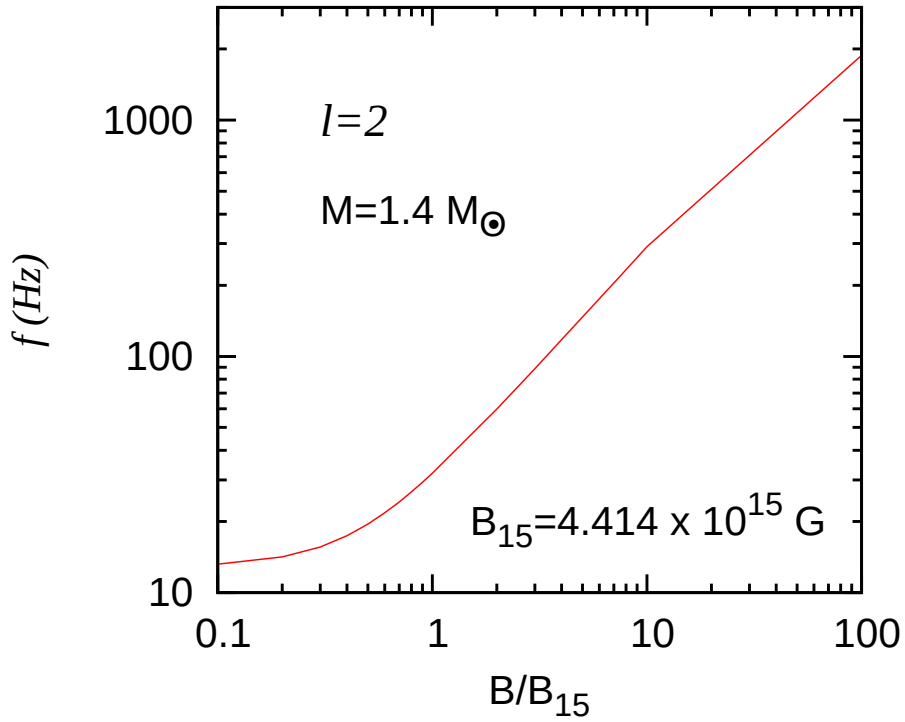

Figure: Fundamental shear modes versus magnetic field

Overtones

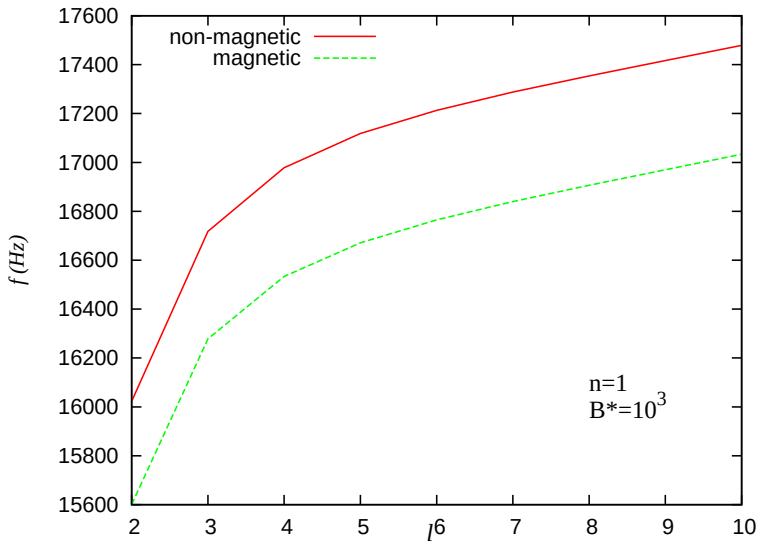
non-magnetic
magnetic
n=1
B*=10^3
f (Hz)
l
17600
17400
17200
17000
16800
16600
16400
16200
16000
15800
15600
2
3
4
5
6
7
8
9
10

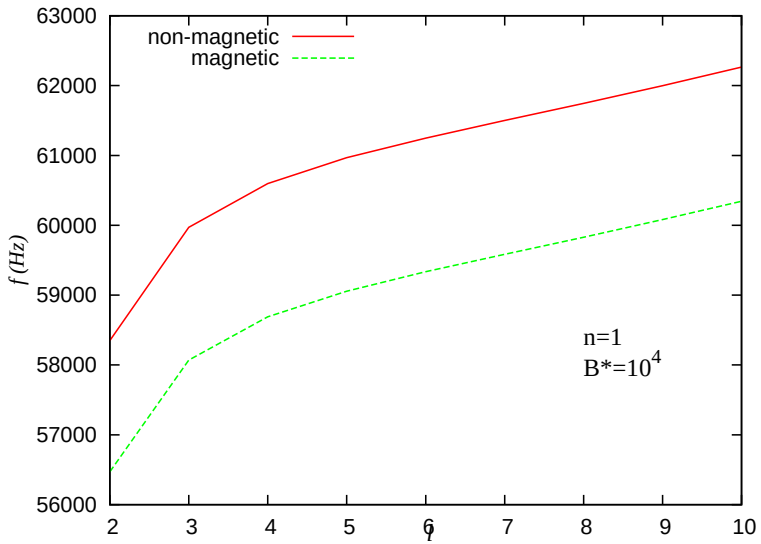
non-magnetic
magnetic
n=1
B*=10^4
f (Hz)
l
63000
62000
61000
60000
59000
58000
57000
56000
2
3
4
5
6
7
8
9
10

SGR 1900+14

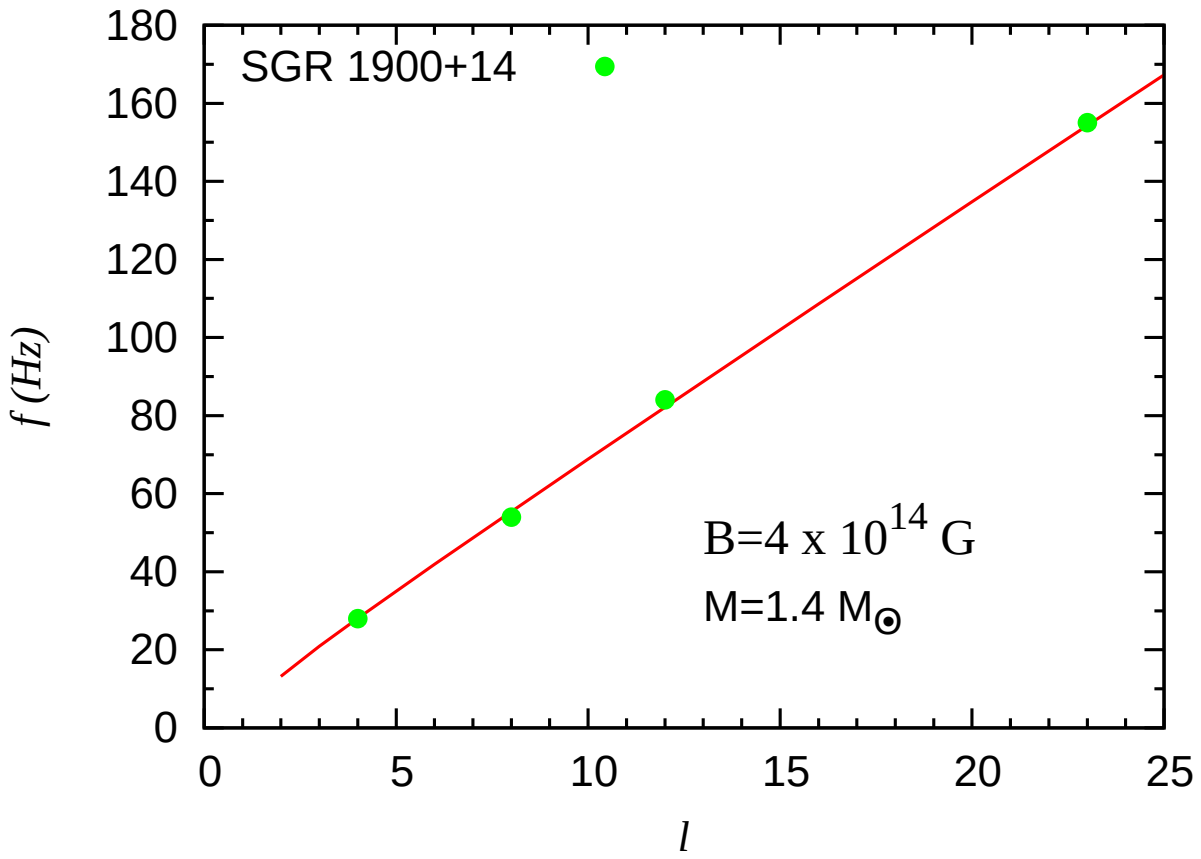

Figure: Comparison with the observed frequencies for SGR 1900+14 .

SGR 1806-20

Observed Frequency (Hz)	Calculated Frequency (Hz)	n	ℓ
18	15	0	2
26	24	0	3
29	32	0	4
93	93	0	12
150	151	0	20
626	626	1	29
1838	1834	2	4

- For SGR 1806-20 the value of magnetic field is $\simeq 8 \times 10^{14}$ G and we assume its mass to be $M = 1.2 M_{\odot}$.
- From the table we see that higher frequencies match well, but lower frequencies are not obtained with satisfactory accuracy.

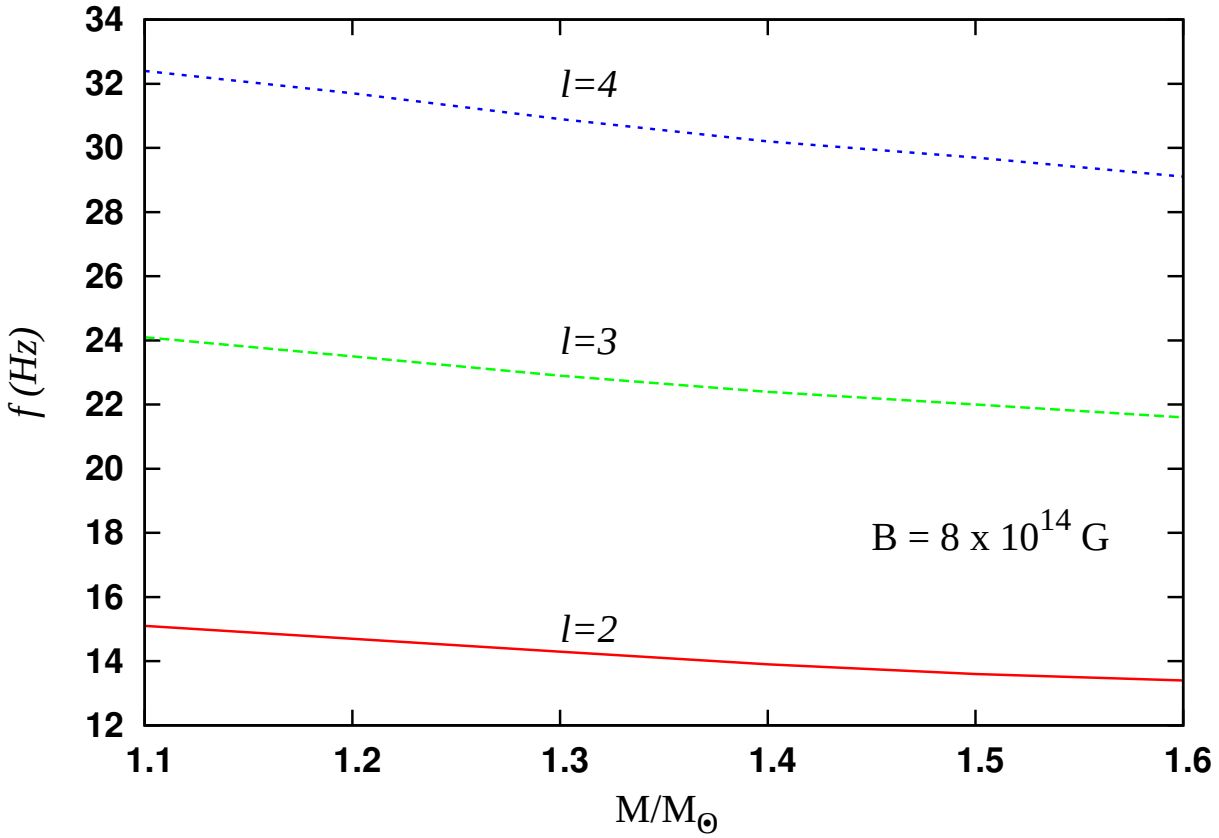

Figure: Variation of frequencies with stellar mass .

R. Nandi, D. Chatterjee and D. Bandyopadhyay, arXiv:1207.3247

Summary & Conclusion

- We have calculated the shear mode frequencies by taking the effects of magnetic fields on the EOS as well as shear modulus of the crust
- It is found that change in shear modulus is not great enough to change the fundamental frequencies. However, it may change the overtones significantly.
- We could successfully reproduce the observed frequencies for SGR 1900+14 and higher frequencies for SGR 1806-20.
- If masses of the SGRs can be obtained by other means, observed frequencies can be used to constraint the EOS.
- In the crusts, electrons were assumed to be uniformly distributed. This needs to be looked at.
- Shear mode calculation will be performed using crust-core coupling.

Thank You